PHYSICAL REVIEW A **96**, 013432 (2017)

Probing degrees of orientation of top molecules with odd-even high-order harmonics

S. J. Yu,[1] W. Y. Li,[2] Y. P. Li,[1] and Y. J. Chen[1,*]
[1]*College of Physics and Information Technology, Shaan'xi Normal University, Xi'an 710119, China*
[2]*School of Mathematics and Science, Hebei GEO University, Shijiazhuang 050031, China*

(Received 3 March 2017; published 31 July 2017)

Molecular orientation has wide applications in physics and chemistry. However, the degree of orientation achieved in experiments is difficult to evaluate, especially when three-dimensional (3D) orientation is involved. We show numerically and analytically that odd-even high-harmonic generation (HHG) from asymmetric molecules is sensitive to both the degree of orientation and the molecular structure. Based on the observations, a simple procedure is proposed to probe the degree of orientation with odd-even HHG, without the need of solving the rotational equation. This procedure can be applied to 3D-oriented top molecules such as polar or nonpolar planar $H_3{}^{2+}$ with high resolution.

DOI: 10.1103/PhysRevA.96.013432

I. INTRODUCTION

Laser-induced molecular alignment has attracted great interest in recent years [1]. It has wide applications ranging from chemical reaction dynamics [2,3] and nanoscale processing [4,5] to high-harmonic spectroscopy (HHS) [6,7] and laser-induced electron diffraction [8–10]. Extending these applications to polar molecules, in addition to alignment, the orientation of the sample also needs to be considered to distinguish the head and the tail of the molecule. The orientation has manifested itself in stereodynamical studies of chemical reactions [11], photoelectron imaging of asymmetric molecular structures [12], probing the electron dynamics of asymmetric molecules with HHS [13–16], and high-harmonic reconstruction of asymmetric orbitals [17,18], etc.

Much effort has been devoted to developing the technique of molecular orientation which is more difficult than molecular alignment. On the whole, present orientation methods are based on the use of a dc field [19]; combinations of electrostatic fields and pulsed nonresonant fields [20]; combination of a rapidly turned-off laser field and an electrostatic field [21]; an IR and UV pulse pair [22]; terahertz laser pulses [23,24]; nonresonant two-color laser fields [25–28]; quantum-state selected molecules in combination with a weak dc field [12,29,30]; two-color ($\omega + 2\omega$) laser fields followed by an ionization-depletion mechanism [13,31]; and a one-color and a delayed two-color nonresonant laser field [16,32]. With these efforts, a high degree of orientation in high gas densities for polar molecules has been possible in experiments [13,16], which facilitates attosecond probing of molecular structure and dynamics.

However, with the great advance of the orientation technique, there is still a difficult question which needs to be solved before a quantitative analysis of orientation-related experimental results can be executed. That is, the evaluation of degree of orientation achieved in experiments. Because accurate calculations of the degree of orientation currently represent a significant challenge [32], it is usually evaluated indirectly. Present procedures for calibrating the degree of orientation include Coulomb explosion imaging [20,27], which assumes that the emitted directions of the fragment ions reflect the directions of the molecular axes just before dissociation of the target; free-induction decay [23,24], which is not proportional to the degree of orientation but to its time derivative; the even-to-odd ratio (the ratio of even to odd harmonic yields) [13], which could be subjected to the interference effect [33]; a comparison of the theoretical harmonic spectra to the experimental ones [32], which needs the calculations of both the harmonic yields and the alignment distribution; and the use of high-harmonic generation (HHG) in ultrashort laser pulses [34], which is applicable for molecules with a large permanent dipole. For top molecules when three-dimensional (3D) orientation is involved, the question becomes more complex. The above procedures cannot be readily generalized to 3D cases where more degrees of freedom need to be manipulated.

In this paper, we demonstrate a procedure for probing the degree of orientation of top molecules with odd-even HHG numerically and analytically. We show that odd-even harmonic yields from asymmetric molecules are dependent on both the molecular structure and the degree of orientation. One can calibrate the degree of orientation using odd-even HHG with considering the influence of the molecular structure. Through this procedure, degrees of orientation for planar molecules $H_3{}^{2+}$ with different configurations are evaluated with high accuracy. This procedure can be applied to more complex top molecules without inversion symmetry, whether polar or nonpolar.

II. CALIBRATING PROCEDURE

It has been shown that there is a close relation between the corresponding dipole $D_{\mathrm{odd\,(even)}}$ and the coherent part of the spectrum $F^{\mathrm{odd\,(even)}}$ for molecules lacking inversion symmetry [17,18]. Generalizing this relation to 3D-oriented cases, we have

$$F^{\mathrm{odd}}(\omega,\theta,\phi) = \sqrt{N(\theta,\phi)}a(\omega)D_{\mathrm{odd}}(\omega,\theta,\phi);$$
$$F^{\mathrm{even}}(\omega,\theta,\phi) = \sqrt{N(\theta,\phi)}a(\omega)D_{\mathrm{even}}(\omega,\theta,\phi). \qquad (1)$$

Here, θ and ϕ are the orientation angles, defined between the laser polarization and a chosen molecular axis. $a(\omega)$ is the spectral amplitude of the continuum electron which is not sensitive to the angles θ and ϕ [6]. $D_{\mathrm{odd\,(even)}}(\omega,\theta,\phi) = \langle \phi_0^{g(u)}(\mathbf{r})|\vec{\mathbf{e}} \cdot \mathbf{r}|e^{i\mathbf{p}\cdot\mathbf{r}}\rangle$ is the dipole associated with the even-parity

---

[*] chenyjhb@gmail.com

2469-9926/2017/96(1)/013432(7)

(odd-parity) component $\phi_0^g(\mathbf{r})$ $[\phi_0^u(\mathbf{r})]$ of the asymmetric molecular orbital $\phi_0(\mathbf{r})$ with $\phi_0(\mathbf{r}) = \phi_0^g(\mathbf{r}) + \phi_0^u(\mathbf{r})$. $\vec{\mathbf{e}} \equiv \vec{\mathbf{e}}(\theta,\phi)$ is the unit vector along the laser polarization. $N(\theta,\phi)$ is the ionization probability, and ω is the emitted photon frequency. In calculating the dipoles $D_{\text{odd (even)}}$, a modified version of plane-wave approximation is used where the Coulomb acceleration of the returning electron is considered [6,17].

Now, we consider the orientation effect. As in [13–15], we assume that the molecules are perfectly aligned and only partially oriented (with n_u molecules pointing up and n_d pointing down); then we have

$$F_{\text{orien}}^{\text{odd}}(\omega,\theta,\phi) = \sqrt{N(\theta,\phi)}a(\omega)D'_{\text{odd}}(\omega,\theta,\phi);$$
$$F_{\text{orien}}^{\text{even}}(\omega,\theta,\phi) = \sqrt{N(\theta,\phi)}a(\omega)D'_{\text{even}}(\omega,\theta,\phi), \tag{2}$$

with $F_{\text{orien}}^{\text{odd (even)}}$ being the odd (even) spectrum associated with imperfect orientation and

$$D'_{\text{odd}}(\omega,\theta,\phi) = n_u D_{\text{odd}}^u(\omega,\theta,\phi) + n_d D_{\text{odd}}^d(\omega,\theta,\phi);$$
$$D'_{\text{even}}(\omega,\theta,\phi) = n_u D_{\text{even}}^u(\omega,\theta,\phi) + n_d D_{\text{even}}^d(\omega,\theta,\phi). \tag{3}$$

Here, the dipoles $D^{u(d)}$ are associated with molecules pointing up (down) with perfect orientation. Due to the symmetry, we have $D_{\text{odd}}^d = D_{\text{odd}}^u$ and $D_{\text{even}}^d = -D_{\text{even}}^u$. Then we obtain

$$F_{\text{orien}}^{\text{odd}}(\omega,\theta,\phi) = (n_u + n_d)\sqrt{N(\theta,\phi)}a(\omega)D_{\text{odd}}^u(\omega,\theta,\phi);$$
$$F_{\text{orien}}^{\text{even}}(\omega,\theta,\phi) = (n_u - n_d)\sqrt{N(\theta,\phi)}a(\omega)D_{\text{even}}^u(\omega,\theta,\phi). \tag{4}$$

When defining the degree of orientation as $\eta = (n_u - n_d)/(n_u + n_d)$, we arrive at

$$\eta^2 = \left| \frac{F_{\text{orien}}^{\text{even}}(\omega,\theta,\phi)}{F_{\text{orien}}^{\text{odd}}(\omega,\theta,\phi)} \frac{D_{\text{odd}}^u(\omega,\theta,\phi)}{D_{\text{even}}^u(\omega,\theta,\phi)} \right|^2 = \zeta \left| \frac{D_{\text{odd}}^u(\omega,\theta,\phi)}{D_{\text{even}}^u(\omega,\theta,\phi)} \right|^2. \tag{5}$$

Here, ζ is the even-to-odd ratio. The above expression explicitly shows the relation between the degree of orientation, the even-to-odd ratio, and the molecular structure. Considering imperfect alignment with the alignment distribution $A(\theta,\phi)$, we also have

$$\eta^2 = \left| \frac{F_{\text{align}}^{\text{even}}(\omega) \int A(\theta,\phi)\sqrt{N(\theta,\phi)}D_{\text{odd}}^u(\omega,\theta,\phi)\sin\theta\, d\theta\, d\phi}{F_{\text{align}}^{\text{odd}}(\omega) \int A(\theta,\phi)\sqrt{N(\theta,\phi)}D_{\text{even}}^u(\omega,\theta,\phi)\sin\theta\, d\theta\, d\phi} \right|^2. \tag{6}$$

Here, $F_{\text{align}}^{\text{odd (even)}} = \int A(\theta,\phi)F_{\text{orien}}^{\text{odd (even)}}(\omega,\theta,\phi)\sin\theta\, d\theta\, d\phi$. In Eqs. (5) and (6), the calculated η depends on the harmonic frequency. As treated in [13,15], one can average the value of η over the harmonics in the whole HHG plateau. Then the averaged degree of orientation independent of the harmonic wavelength can be obtained. It should be mentioned that a similar result to Eq. (2) has been obtained in [16,32], where odd-even HHG from linear molecules is studied and the degree of orientation is evaluated with comparing the analytical results of odd-even HHG spectra to the experimental ones. In addition, in comparison with Eq. (5), the relation $\eta^2 = \zeta$ has also been used to calibrate the degree of orientation with the even-to-odd ratio in [13,15]. As mentioned in [13,15], the method of only using the even-to-odd ratio merely provides an upper bound for the degree of orientation.

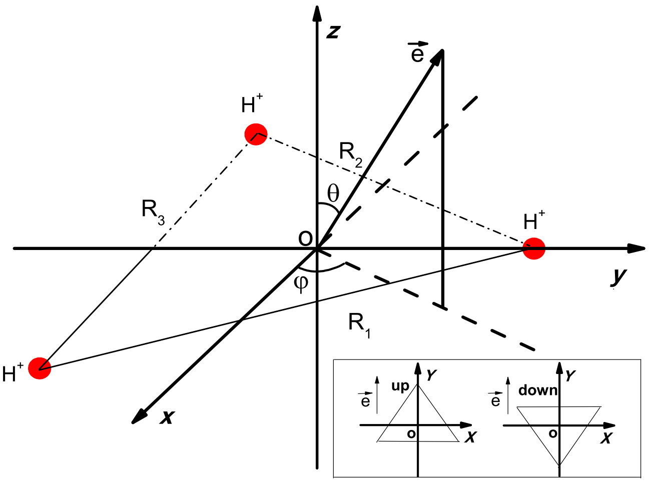

FIG. 1. A sketch of the molecular geometry and the coordinate system used in 3D simulations (in atomic units of $\hbar = e = m_e = 1$). The $\text{H}_3{}^{2+}$ molecule is located in the xoy plane. The y axis goes through one H nucleus and the center of mass of the molecular system coincides with the origin of the coordinate system o. θ denotes the angle between the laser polarization and the z axis (i.e., the zenith angle), and ϕ is the azimuthal angle of the laser polarization. R_1, R_2, and R_3 are the internuclear separations. The insets show the cases of molecules pointing up and down.

III. APPLICATION

Below, we will apply the above procedure to planar molecules $\text{H}_3{}^{2+}$ [35] with different configurations. The planar $\text{H}_3{}^{2+}$ is the simplest top molecule which can be used as a benchmark for more complex ones. In addition, by changing the molecular configurations through adjusting the internuclear distances of the system, we can change the value of the permanent dipole. These allow us to explore the applicability of our procedure for both polar and nonpolar top molecules.

A. Planar $\text{H}_3{}^{2+}$ model

The Hamiltonian of the planar molecule $\text{H}_3{}^{2+}$ studied is $H(t) = \mathbf{p}^2/2 + V(\mathbf{r}) + \mathbf{r}\cdot\mathbf{E}(t)$ (in atomic units of $\hbar = e = m_e = 1$). We assume that the $\text{H}_3{}^{2+}$ molecule is located in the xoy plane and the laser field is linearly polarized with the orientation $\Omega = (\theta,\phi)$. A sketch of the coordinate system used in our 3D simulations is presented in Fig. 1. The potential used here has the form of $V(\mathbf{r}) = -Z/\sqrt{\xi + (\mathbf{r}-\mathbf{R}_a)^2} - Z/\sqrt{\xi + (\mathbf{r}-\mathbf{R}_b)^2} - Z/\sqrt{\xi + (\mathbf{r}-\mathbf{R}_c)^2}$. Here $Z = 1$ is the effective charge, and $\mathbf{R}_a$, $\mathbf{R}_b$, and $\mathbf{R}_c$ are the vectors between the origin and these three nuclei. $\xi = 0.5$ is the smoothing parameter.

$\mathbf{E}(t) = \vec{\mathbf{e}}E(t)$ with $E(t) = f(t)\mathcal{E}\sin\omega_0 t$ is the external electric field. $\vec{\mathbf{e}} \equiv \vec{\mathbf{e}}(\theta,\phi) = (\sin\theta\,\cos\phi, \sin\theta\,\sin\phi, \cos\theta)$ is the unit vector along the laser polarization. ω_0 is the laser frequency and $f(t)$ is the envelope function. $\mathcal{E}$ is the laser amplitude relating to the peak laser intensity I. We use trapezoidally shaped laser pulses with a total duration of ten optical cycles and linear ramps of three optical cycles. The time-dependent Schrödinger equation (TDSE) of $i\dot{\Psi}(t) = H(t)\Psi(t)$ is solved numerically using the spectral method [36], with 2048 time steps in each laser cycle. In practical calculations, the coordinate system is rotated in such a manner that the x axis coincides with the laser polarization, allowing the use of different grids for different dimensions. We work with a grid of $L_x \times L_y \times L_z = 410 \times 51 \times 51$ a.u. The space steps used are $\Delta x = \Delta y = \Delta z = 0.4$ a.u. The laser parameters used are $I = 8 \times 10^{14}$ W/cm^2 and $\lambda = 800$ nm. Once the TDSE wave function $\psi(t)$ is obtained, the coherent part of the HHG spectrum at the orientation $\Omega = (\theta,\phi)$ for one odd or even harmonic ω can be evaluated using [37]

$$F(\omega,\theta,\phi) = \int D(\theta,\phi)e^{i\omega t}dt, \tag{7}$$

where $D(\theta,\phi) = \langle \psi(t)|\vec{\mathbf{e}} \cdot \nabla V|\psi(t)\rangle$ is the TDSE dipole acceleration. Considering imperfect orientation with n_u (n_d) molecules pointing up (down), we have

$$F_{\mathrm{orien}}(\omega,\theta,\phi) = \int [n_u D_u(\theta,\phi) + n_d D_d(\theta,\phi)]e^{i\omega t}dt. \tag{8}$$

Here, $D_{u(d)}$ is the dipole acceleration related to the case of molecules pointing up (down), as shown in the insets in Fig. 1.

B. Odd-even spectra and dipoles

In our simulations, the HHG from planar $H_3{}^{2+}$ with different configurations shows the strong emission of even harmonics for large and intermediate angles θ and for all of angles ϕ (but $\phi = 60^\circ$ for the equilateral-triangle configuration due to the geometry of the molecule). On the whole, the even harmonics diminish with the decrease of the angle θ and they disappear for $\theta = 0^\circ$. Moreover, the even harmonics are stronger for $\phi = 90^\circ$ than for $\phi = 0^\circ$. In particular, the emission of even harmonics depends strongly on the degree of orientation η, and this emission is stronger for larger η. In contrast, the odd-harmonic emission is not sensitive to η.

In one case, in Fig. 2, we plot the odd-even HHG spectra obtained using Eq. (8) for different η, at $\theta = 45^\circ$ and $\phi = 40^\circ$ with an equilateral-triangle configuration. The corresponding dipoles of Eq. (3) are also presented here, where the analytical expression of $\phi_0(\mathbf{r})$ for $H_3{}^{2+}$ is obtained with a linear combination of atomic orbital and molecular orbital approximations [17]. From Fig. 2, we observe a one-to-one correspondence between η-dependent odd-even spectra and dipoles. The relative yields of odd versus even harmonics in the HHG plateau region are well predicted by relevant dipoles at different η, implying the applicability of Eq. (2) in 3D-oriented cases. Nevertheless, there remains an obvious difference between relevant spectra and dipoles. As the odd dipoles show a striking minimum arising from the effect of two-center interference [17,37], this minimum is not remarkable in the odd spectra. As discussed in [38,39], in the interference-dominating energy regions, there are different recombination routes contributing to the emission of one odd or even harmonic. As a result, the HHG spectra of asymmetric molecules usually do not show a striking minimum. For the use of Eq. (5) to calibrate the value of η, we treat the minimum in the odd dipole with a Gaussian fit. The treated odd dipoles are plotted using dashed-dotted curves in the lower row of Fig. 2.

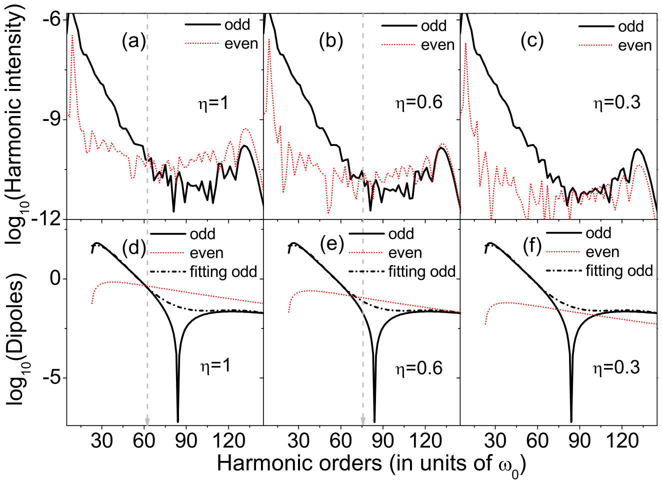

FIG. 2. Comparisons of odd-even HHG spectra of Eq. (8) [(a)–(c)] and dipoles $|D'_{\mathrm{odd\,(even)}}|^2$ of Eq. (3) [(d)–(f)] for planar molecules $H_3{}^{2+}$ with the orientation of $(\theta = 45^\circ, \phi = 40^\circ)$ and internuclear distances of $R_1 = R_2 = R_3 = 2$ a.u. at different degrees of orientation η. In (d)–(f), the black dashed-dotted curves show the rectified odd dipoles with a Gaussian fit, which eliminates the interference minima in these dipoles.

C. Calibrating degrees of orientation

Using the odd-even HHG spectra and the treated dipoles as discussed in Fig. 2, next we calibrate the degree of orientation with Eq. (5). For each case of the spectra, the calculated η by Eq. (5) is averaged over the harmonics in the whole HHG plateau. Relevant results are presented in Fig. 3. Here, we show two typical cases for the molecular configuration: equilateral triangle (a nonpolar $H_3{}^{2+}$) in Figs. 3(a) and 3(c), and scalene triangle (the polar one) in Figs. 3(b) and 3(d). We also vary the value of the orientation $\Omega = (\theta,\phi)$. For comparison, we present our results in two different manners. In Figs. 3(a) and 3(b), the calibrated values of η by Eq. (5) are plotted as a

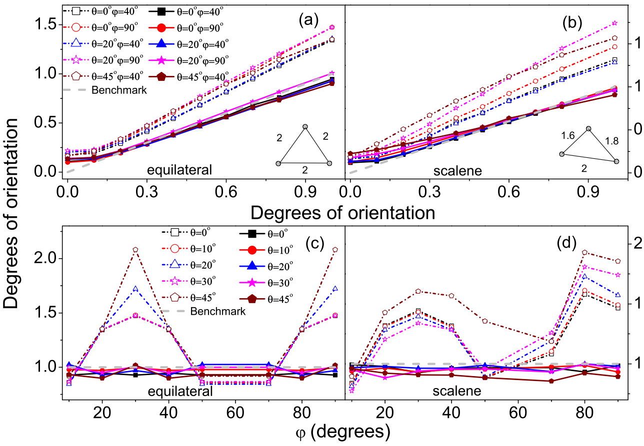

FIG. 3. Degrees of orientation obtained with Eq. (5) (solid symbols) as a function of the actual degree of orientation used in 3D TDSE [(a),(b)] and a function of the angle ϕ with perfect orientation of $\eta = 1$ [(c),(d)] for different orientations $\Omega = (\theta,\phi)$, and for different molecular configurations: equilateral triangle with $R_1 = R_2 = R_3 = 2$ a.u. [(a),(c)] and scalene triangle with $R_1 = 2$ a.u., $R_2 = 1.8$ a.u., and $R_3 = 1.6$ a.u. [(b),(d)]. For comparison, the degrees of orientation obtained using even-to-odd ratio (open symbols) are also shown. Gray dashed curves represent the exact results serving as a benchmark.

function of the actual value of η used in 3D TDSE simulations. In Figs. 3(c) and 3(d), the actual value of η is fixed at $\eta = 1$ (perfect orientation); the calibrated values of η by Eq. (5) are plotted as a function of the angle ϕ.

These results in Fig. 3 are encouraging in that in both polar and nonpolar cases, the degrees of orientation calibrated by Eq. (5) (curves with solid symbols) agree well with the exact results (gray-dashed). By comparison, the values of η evaluated with even-to-odd ratio (curves with hollow symbols), where the expression of $\eta^2 = \zeta$ is used and the influence of the dipoles is omitted, differ remarkably from the exact ones. This difference seems more striking for the polar case in Figs. 3(b) and 3(d). On the whole, the evaluation with even-to-odd ratio ζ overestimates (underestimates) the value of η as the emission of even harmonics is stronger (weaker) than the odd one.

D. Alignment effect

So far, our discussions are based on perfect alignment of the sample. In real experiments, perfect alignment is also impossible. Below, we explore the applicability of the calibrating procedure of Eq. (6) where the alignment distribution $A(\theta,\phi)$ is considered. The laser field $\mathbf{E}(t)$ always can be divided into the component $E_z(t) = E(t)\cos\theta$ along the z axis, and the component $E_{xy}(t) = E(t)\sin\theta$ located in the xoy plane. For the plane molecule $H_3{}^{2+}$, it is the component $E_{xy}(t)$ that induces the emission of even harmonics. For this reason, we simplify our discussions by assuming that the laser field $\mathbf{E}(t)$ is located in the xoy plane ($\theta = 90^\circ$) and $A(\theta,\phi) \equiv A(\phi)$. With these assumptions, Eq. (6) can be rewritten as

$$\eta^2 = \left| \frac{F^{\mathrm{even}}_{\mathrm{align}}(\omega) \int_0^\pi A(\phi)\sqrt{N(\theta,\phi)}D^u_{\mathrm{odd}}(\omega,\theta,\phi)d\phi}{F^{\mathrm{odd}}_{\mathrm{align}}(\omega) \int_0^\pi A(\phi)\sqrt{N(\theta,\phi)}D^u_{\mathrm{even}}(\omega,\theta,\phi)d\phi} \right|^2. \quad (9)$$

Here, $F^{\mathrm{odd\,(even)}}_{\mathrm{align}}(\omega) = \int_0^\pi A(\phi)F^{\mathrm{odd\,(even)}}_{\mathrm{orien}}(\omega,\theta,\phi)d\phi$, and the angle θ in the above expression is fixed at $\theta = 90^\circ$. Generally, the alignment distribution can be calculated through numerical solution of the TDSE [32]. Here, to study the influence of molecular alignment on the calibrating procedure for the degree of orientation, as in [40], we assume that the alignment distribution $A(\phi)$ has the form of $A(\phi) = M(1 + a/\sqrt{\cos^2\phi + b^2\sin^2\phi})$, where a and b are parameters that are adjusted to produce the desired degree of alignment and M is a normalization constant. Similar treatments have been used in [41].

Let us discuss $A(\phi)$ in somewhat more detail. The alignment distribution $A(\phi)$ gives the weight of the aligned ensemble at angle ϕ, when in real experiments, the ensemble can only partly be aligned with a preference at one certain angle. The range of the angle ϕ is from 0 to 2π for the planar molecule. When calculating the odd-even HHG, the situation is similar for these two cases of ϕ and $\phi + \pi$. Specifically, the case of molecules pointing up at angle ϕ corresponds to the case of molecules pointing down at $\phi + \pi$ and vice versa. For this reason, in Eq. (9), the integral is taken from 0 to π.

We consider the equilateral-triangle case with the orientation of ($\theta = 90^\circ, \phi = 90^\circ$) at which the emission of even harmonics is the most striking for the planar molecule $H_3{}^{2+}$. These calculated distributions of $A(\phi)$ for different degrees of alignment defined using $\langle\sin^2\phi\rangle$ are presented in Fig. 4(a).

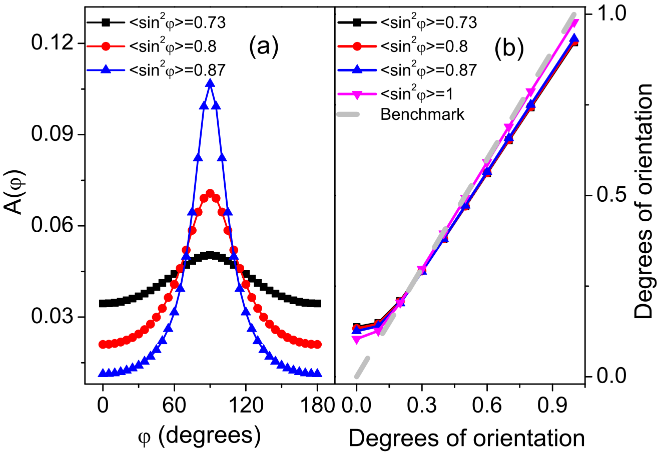

FIG. 4. Alignment distributions (a) and degrees of orientation obtained with Eq. (9) (b) for different degrees of alignment defined using $\langle\sin^2\phi\rangle$. The gray dashed curve in (b) represents the exact result serving as a benchmark.

Note, for this present case, the distributions are sharper around $\phi = 90^\circ$ for larger values of $\langle\sin^2\phi\rangle$. For random alignment, $\langle\sin^2\phi\rangle = 0.67$.

The values of η calibrated through Eq. (9) with these calculated distributions $A(\phi)$ are presented in Fig. 4(b). One can observe that the calibrated results are not sensitive to the degree of alignment. They are very near to each other, and to the exact one (gray dashed) as well as the result of perfect orientation (down triangle). Since the alignment distribution gives weight to the contribution of each angle ϕ at which Eq. (5) works well, one can expect that Eq. (9) relating to the sum of the weighted contributions is also able to provide an applicable prediction of the degree of orientation.

We have also extended our simulations to other laser parameters and other internuclear distances. In all cases, this above calibrating procedure gives a good prediction of the degree of orientation. The macroscopic propagation effect of the HHG signal is also approximately considered with averaging the TDSE dipole acceleration over different laser intensities and assuming a thin gas jet used in experiments [42]. Relevant results are shown in Fig. 5. Here, we plot the odd-even HHG spectra of $H_3{}^{2+}$ of an equilateral-triangle configuration with the orientation of ($\theta = 90^\circ$ and $\phi = 90^\circ$) and the degree of orientation of $\eta = 1$. In Fig. 5(a), we plot the spectra obtained with averaging the TDSE dipole acceleration over different laser intensities of $I = 7\times10^{14}$ W/cm^2 to $I = 9\times10^{14}$ W/cm^2. For comparison, in Fig. 5(b), we also plot the spectra obtained at the laser intensity of $I = 8\times10^{14}$ W/cm^2. Relevant odd-even dipoles of Eq. (3) are shown in Fig. 5(c). One can observe that the relative yields of odd versus even harmonics of the averaged spectra in Fig. 5(a) are consistent with those in Fig. 5(b), and are in agreement with the predictions of the relevant dipoles in Fig. 5(c). The values of η calibrated with the averaged spectra (open symbols) and the spectra at $I = 8\times10^{14}$ W/cm^2 (solid symbols) are presented in Fig. 5(d). It can be observed that the open-symbol curve agrees with the solid-symbol curve basically, when the actual degree of orientation used in 3D TDSE calculations is near to or larger than 0.2. The above comparisons imply that when the

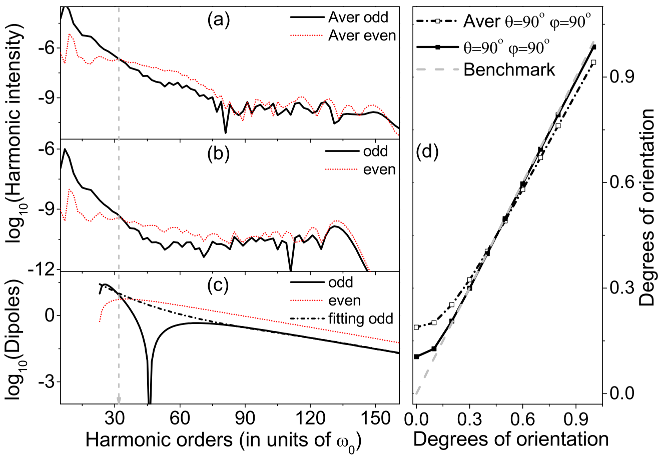

FIG. 5. Comparisons of odd-even HHG spectra of Eq. (8) averaged over different laser intensities of $I = 7\times10^{14}$ W/cm^2 to $I = 9\times10^{14}$ W/cm^2 (a) and at the laser intensity of $I = 8\times10^{14}$ W/cm^2 (b), for planar molecules $H_3{}^{2+}$ with the orientation of $(\theta = 90^\circ, \phi = 90^\circ)$, the degree of orientation of $\eta = 1$, and internuclear distances of $R_1 = R_2 = R_3 = 2$ a.u. In (c), the corresponding odd-even dipoles $|D'_{\text{odd (even)}}|^2$ of Eq. (3) are also shown, where the black dashed-dotted curves show the rectified odd dipoles with a Gaussian fit, as introduced in Fig. 2. In (d), the corresponding degrees of orientation of Eq. (5) obtained with the averaged spectra (open symbols) and the spectra at $I = 8\times10^{14}$ W/cm^2 (solid symbols), are also shown. The gray dashed curve in (d) represents the exact result serving as a benchmark.

gas jet is thin in experiments, it is possible to use the odd-even HHG signals to calibrate the degree of orientation with the procedure suggested here.

E. Multielectron effects and Coulomb effects

Above, we have presented a procedure for calibrating the degree of orientation using the even-to-odd ratio and considering the molecular structure. However, there are limitations in our discussions.

Firstly, the simple planar molecule $H_3{}^{2+}$ is used as the target in our simulations, which allows the solution of the TDSE for one electron with a high accuracy and allows the description of odd-even HHG using Eq. (1) of the simplified version of the Lewenstein model [43]. However, the $H_3{}^{2+}$ molecule is not an ideal candidate for a feasible experimental HHG study. Furthermore, the ground-state wave function of $H_3{}^{2+}$ is mainly composed of three overlapping s orbitals, which carries little orbital angular momentum. As such, many effects of the Coulomb potential on the continuum electrons such as shape resonances, which require contributions from partial waves with higher angular momentum in the photoionization continuum, are minimized.

For complex multielectron top molecules which are experimentally feasible (e.g., methyl halides [44]), multiple ionic states will also be populated by strong-field ionization and a sum needs to be included in Eq. (1) to sum over all states of the cation. Furthermore, the electric field can transfer population between the electronic states of the cation, which also has to be included. In this situation, Eq. (1) approximately has the form of

$$F^{\text{odd}}(\omega,\theta,\phi) = \sum_i \sqrt{N_i(\theta,\phi)}a_i(\omega)D_{i,\text{odd}}(\omega,\theta,\phi);$$
$$F^{\text{even}}(\omega,\theta,\phi) = \sum_i \sqrt{N_i(\theta,\phi)}a_i(\omega)D_{i,\text{even}}(\omega,\theta,\phi), \quad (10)$$

where the sum is over all of the ionic and electronic states. The term $D_{i,\text{odd (even)}}$ denotes the odd (even) component of the dipole of the ith ionic or electronic state. The term $a_i(\omega)$ is the corresponding spectral amplitude and $N_i(\theta,\phi)$ is the corresponding ionization rate. Accordingly, Eq. (5) has the form of

$$\eta^2 = \zeta\left|\frac{\sum_i \sqrt{N_i(\theta,\phi)}a_i(\omega)D^u_{i,\text{odd}}(\omega,\theta,\phi)}{\sum_i \sqrt{N_i(\theta,\phi)}a_i(\omega)D^u_{i,\text{even}}(\omega,\theta,\phi)}\right|^2, \quad (11)$$

and Eq. (6) can be rewritten as

$$\eta^2 = \left|\frac{F^{\text{even}}_{\text{align}}(\omega)\,\sum_i \int A(\theta,\phi)N'_i a_i(\omega)D^u_{i,\text{odd}}(\omega,\theta,\phi)\sin\theta\, d\theta\, d\phi}{F^{\text{odd}}_{\text{align}}(\omega)\,\sum_i \int A(\theta,\phi)N'_i a_i(\omega)D^u_{i,\text{even}}(\omega,\theta,\phi)\sin\theta\, d\theta\, d\phi}\right|^2. \quad (12)$$

Here, $N'_i \equiv \sqrt{N_i(\theta,\phi)}$. The spectral amplitude $a_i(\omega)$ can be calculated [16,32] in the strong-field approximation (SFA) [43] with an additional, Stark-effect-induced alignment-dependent phase factor [45,46]. The strong-field ionization rate $N_i(\theta,\phi)$ of multielectron systems can be calculated using the time-dependent mixed orbital and grid method [47]. However, the knowledge of the dipole D_i is absent in many cases (the extraction of the dipole is the aim of most HHG spectroscopy experiments) and the calculations of strong-field ionization rates of multielectron molecules with considering the coupling between multiple ionic channels also present a challenge at present [47]. These limit the use of the proposed procedure in the paper to probe the degree of orientation of complex top molecules. Based on the above discussions, we expect that the procedure proposed in the paper is more applicable for (1) top molecules for which the knowledge of the dipole is acquirable and (2) relatively low laser intensities and long laser wavelengths at which the contributions of the ionic or electronic states to odd-even HHG can be minimized.

Secondly, the plane-wave (PW) approximation is used in calculating the dipole $D_{\text{odd (even)}}$ analytically in this paper. The PW has limitations in describing continuum electrons whenever the influence of the Coulomb potential on the recombining photoelectron wave packet cannot be neglected (see, e.g., [48]). Instead of the PW approximation, the Coulomb wave (CW) [49–51] or the incoming scattering wave [48] which considers the influence of the parent ion field on the continuum electrons has been widely used in SFA.

In this paper, a simple HHG model of Eq. (1) is used to describe the generation mechanism of odd-even HHG. In this model, the odd-even HHG spectra are shown to be closely related to the odd-even bound-continuum transition dipoles $D_{\mathrm{odd\,(even)}}$. One can divide the bound-continuum transition dipole D into odd and even components with the PW approximation. When the CW is used, the bound-continuum transition dipole D cannot be divided into odd-even components directly and a phase rotation of the CW dipole is needed to relate the CW dipole to the PW one. This phase is obtained with comparing the reconstructed molecular orbital with the exact one, as discussed in detail in [49]. Since this phase has to be introduced into relevant calculations as a parameter when the CW is used, in the present paper, we use a modified version of the PW approximation in our calculations. In the modified PW approximation, the effective momentum $p_k = \sqrt{p^2 + 2I_p}$ that considers the Coulomb acceleration is used instead of the general one p, as in [6,17,18,37]. The applicability of the modified PW approximation has been explored in [52]. On the whole, this approximation is more applicable for electrons with higher energy. In [18], it has also been shown that the reconstructed molecular orbital obtained with the modified PW is similar to the CW one. However, there are still limitations for the modified PW approximation where the Coulomb effect is not considered fully. For example, the disagreement in Fig. 2 between the odd dipole and harmonic intensity, which had to be smoothed out by a Gaussian fit, might exactly be a result of these limitations. To describe the details of odd-even HHG spectra, a developed odd-even HHG model that fully considers the Coulomb effect is also needed.

IV. CONCLUSIONS

In summary, we have shown a procedure for calibrating the degree of orientation of asymmetric molecules with odd-even HHG, where the influence of the molecular structure is considered. This procedure can be applied to 3D-oriented top molecules which lack inversion symmetry, without the need of solving 3D TDSE. Particularly, it is applicable for both polar and nonpolar top molecules, opening the possibility for a wide range of applications. The influence of Coulomb effects, multielectron effects, and the macroscopic propagation effect on this proposed procedure is also discussed. As the degree of orientation plays an important role in many orientation-related processes in photochemistry and attosecond science, our work gives suggestions on relevant experiments.

ACKNOWLEDGMENTS

This work was supported by the National Natural Science Foundation of China (Grants No. 11274090 and No. 11404259), the Youth Foundation of Hebei Province Education Department (Grant No. QN2017028), and the Fundamental Research Funds for the Central Universities (Grant No. SNNU GK201403002).

[1] H. Stapelfeldt and T. Seideman, *Colloquium*: Aligning molecules with strong laser pulses, Rev. Mod. Phys. **75**, 543 (2003).

[2] T. Suzuki, S. Minemoto, T. Kanai, and H. Sakai, Optimal Control of Multiphoton Ionization Processes in Aligned I_2 Molecules with Time-Dependent Polarization Pulses, Phys. Rev. Lett. **92**, 133005 (2004).

[3] I. V. Litvinyuk, K. F. Lee, P. W. Dooley, D. M. Rayner, D. M. Villeneuve, and P. B. Corkum, Alignment-Dependent Strong Field Ionization of Molecules, Phys. Rev. Lett. **90**, 233003 (2003).

[4] T. Seideman, Molecular optics in an intense laser field: A route to nanoscale material design, Phys. Rev. A **56**, R17 (1997).

[5] H. Stapelfeldt, H. Sakai, E. Constant, and P. B. Corkum, Deflection of Neutral Molecules using the Nonresonant Dipole Force, Phys. Rev. Lett. **79**, 2787 (1997).

[6] J. Itatani, J. Levesque, D. Zeidler, H. Niikura, H. Pepin, J. C. Kieffer, P. B. Corkum, and D. M. Villeneuve, Tomographic imaging of molecular orbitals, Nature (London) **432**, 867 (2004).

[7] H. J. Wörner, J. B. Bertrand, D. V. Kartashov, P. B. Corkum, and D. M. Villeneuve, Following a chemical reaction using high-harmonic interferometry, Nature (London) **466**, 604 (2010).

[8] T. Zuo, A. D. Bandrauk, and P. B. Corkum, Laser-induced electron diffraction: A new tool for probing ultrafast molecular dynamics, Chem. Phys. Lett. **259**, 313 (1996).

[9] M. Meckel, D. Comtois, D. Zeidler, A. Staudte, D. Pavičić, H. C. Bandulet, H. Pépin, J. C. Kieffer, R. Dörner, D. M. Villeneuve, and P. B. Corkum, Laser-induced electron tunneling and diffraction, Science **320**, 1478 (2008).

[10] C. I. Blaga, J. Xu, A. D. DiChiara, E. Sistrunk, K. Zhang, P. Agostini, T. A. Miller, L. F. DiMauro, and C. D. Lin, Imaging ultrafast molecular dynamics with laser-induced electron diffraction, Nature (London) **483**, 194 (2012).

[11] T. P. Rakitzis, A. J. van den Brom, and M. H. M. Janssen, Directional dynamics in the photodissociation of oriented molecules, Science **303**, 1852 (2004).

[12] L. Holmegaard, J. L. Hansen, L. Kalhøj, S. L. Kragh, H. Stapelfeldt, F. Filsinger, J. Küpper, G. Meijer, D. Dimitrovski, M. Abu-samha, C. P. J. Martiny, and L. B. Madsen, Photoelectron angular distributions from strong-field ionization of oriented molecules, Nat. Phys. **6**, 428 (2010).

[13] E. Frumker, C. T. Hebeisen, N. Kajumba, J. B. Bertrand, H. J. Wörner, M. Spanner, D. M. Villeneuve, A. Naumov, and P. B. Corkum, Oriented Rotational Wave-Packet Dynamics Studies via High Harmonic Generation, Phys. Rev. Lett. **109**, 113901 (2012).

[14] P. M. Kraus, A. Rupenyan, and H. J. Wörner, High-Harmonic Spectroscopy of Oriented OCS Molecules: Emission of Even and Odd Harmonics, Phys. Rev. Lett. **109**, 233903 (2012).

[15] E. Frumker, N. Kajumba, J. B. Bertrand, H. J. Wörner, C. T. Hebeisen, P. Hockett, M. Spanner, S. Patchkovskii, G. G. Paulus, D. M. Villeneuve, A. Naumov, and P. B. Corkum, Probing Polar Molecules with High Harmonic Spectroscopy, Phys. Rev. Lett. **109**, 233904 (2012).

[16] P. M. Kraus, D. Baykusheva, and H. J. Wörner, Two-Pulse Field-Free Orientation Reveals Anisotropy of Molecular Shape Resonance, Phys. Rev. Lett. **113**, 023001 (2014).

[17] Y. J. Chen and B. Zhang, Tracing the structure of asymmetric molecules from high-order harmonic generation, Phys. Rev. A **84**, 053402 (2011).

[18] Y. J. Chen, L. B. Fu, and J. Liu, Asymmetric Molecular Imaging through Decoding Odd-Even High-Order Harmonics, Phys. Rev. Lett. **111**, 073902 (2013).

[19] B. Friedrich and R. Herschbach, Spatial orientation of molecules in strong electric fields and evidence for pendular states, Nature (London) **353**, 412 (1991).

[20] H. Sakai, S. Minemoto, H. Nanjo, H. Tanji, and T. Suzuki, Controlling the Orientation of Polar Molecules with Combined Electrostatic and Pulsed, Nonresonant Laser Fields, Phys. Rev. Lett. **90**, 083001 (2003).

[21] A. Goban, S. Minemoto, and H. Sakai, Laser-Field-Free Molecular Orientation, Phys. Rev. Lett. **101**, 013001 (2008).

[22] A. V. Sokolov, K. K. Lehmann, M. O. Scully, and D. Herschbach, Orienting molecules via an IR and UV pulse pair: Implications for coherent Raman spectroscopy, Phys. Rev. A **79**, 053805 (2009).

[23] S. Fleischer, Y. Zhou, R. W. Field, and K. A. Nelson, Molecular Orientation and Alignment by Intense Single-Cycle THz Pulses, Phys. Rev. Lett. **107**, 163603 (2011).

[24] P. Babilotte, K. Hamraoui, F. Billard, E. Hertz, B. Lavorel, O. Faucher, and D. Sugny, Observation of the field-free orientation of a symmetric-top molecule by terahertz laser pulses at high temperature, Phys. Rev. A **94**, 043403 (2016).

[25] M. J. J. Vrakking and S. Stolte, Coherent control of molecular orientation, Chem. Phys. Lett. **271**, 209 (1997).

[26] T. Kanai and H. Sakai, Numerical simulations of molecular orientation using strong, nonresonant, two-color laser fields, J. Chem. Phys. **115**, 5492 (2001).

[27] S. De, I. Znakovskaya, D. Ray, F. Anis, Nora G. Johnson, I. A. Bocharova, M. Magrakvelidze, B. D. Esry, C. L. Cocke, I. V. Litvinyuk, and M. F. Kling, Field-Free Orientation of CO Molecules by Femtosecond Two-Color Laser Fields, Phys. Rev. Lett. **103**, 153002 (2009).

[28] K. Oda, M. Hita, S. Minemoto, and H. Sakai, All-Optical Molecular Orientation, Phys. Rev. Lett. **104**, 213901 (2010).

[29] L. Holmegaard, J. H. Nielsen, I. Nevo, H. Stapelfeldt, F. Filsinger, J. Küpper, and G. Meijer, Laser-Induced Alignment and Orientation of Quantum-State-Selected Large Molecules, Phys. Rev. Lett. **102**, 023001 (2009).

[30] O. Ghafur, A. Rouzée, A. Gijsbertsen, W. K. Siu, S. Stolte, and M. J. J. Vrakking, Impulsive orientation and alignment of quantum-state-selected NO molecules, Nat. Phys. **5**, 289 (2009).

[31] M. Spanner, S. Patchkovskii, E. Frumker, and P. Corkum, Mechanisms of Two-Color Laser-Induced Field-Free Molecular Orientation, Phys. Rev. Lett. **109**, 113001 (2012).

[32] P. M. Kraus, D. Baykusheva, and H. J. Wörner, Two-pulse orientation dynamics and high-harmonic spectroscopy of strongly-oriented molecules, J. Phys. B **47**, 124030 (2014).

[33] B. Zhang, S. Yu, Y. Chen, X. Jiang, and X. Sun, Time-resolved dynamics of odd and even harmonic emission from oriented asymmetric molecules, Phys. Rev. A **92**, 053833 (2015).

[34] Y. Z. Shi, B. Zhang, W. Y. Li, S. J. Yu, and Y. J. Chen, Probing degrees of orientation of polar molecules with harmonic emission in ultrashort laser pulses, Phys. Rev. A **95**, 033406 (2017).

[35] E. Lötstedt and K. Midorikawa, Laser-induced electron localization in a triatomic molecular ion, Phys. Rev. A **88**, 041402(R) (2013).

[36] M. D. Feit, J. A. Fleck, Jr., and A. Steiger, Solution of the Schrödinger equation by a spectral method, J. Comput. Phys. **47**, 412 (1982).

[37] M. Lein, N. Hay, R. Velotta, J. P. Marangos, and P. L. Knight, Role of the Intramolecular Phase in High-Harmonic Generation, Phys. Rev. Lett. **88**, 183903 (2002).

[38] B. Zhang, Y. Chen, X. Jiang, and X. Sun, Identifying the interference effect in different harmonic-emission channels from oriented asymmetric molecules, Phys. Rev. A **88**, 053428 (2013).

[39] S. Yu, B. Zhang, Y. Li, S. Yang, and Y. Chen, Ellipticity of odd-even harmonics from oriented asymmetric molecules in strong linearly polarized laser fields, Phys. Rev. A **90**, 053844 (2014).

[40] D. Pavičić, K. F. Lee, D. M. Rayner, P. B. Corkum, and D. M. Villeneuve, Direct Measurement of the Angular Dependence of Ionization for N_2, O_2, and CO_2 in Intense Laser Fields, Phys. Rev. Lett. **98**, 243001 (2007).

[41] A. Rupenyan, J. B. Bertrand, D. M. Villeneuve, and H. J. Wörner, All-Optical Measurement of High-Harmonic Amplitudes and Phases in Aligned Molecules, Phys. Rev. Lett. **108**, 033903 (2012).

[42] S. Beaulieu, S. Camp, D. Descamps, A. Comby, V. Wanie, S. Petit, F. Légaré, K. J. Schafer, M. B. Gaarde, F. Catoire, and Y. Mairesse, Role of Excited States in High-Order Harmonic Generation, Phys. Rev. Lett. **117**, 203001 (2016).

[43] M. Lewenstein, Ph. Balcou, M. Yu. Ivanov, A. L'Huillier, and P. B. Corkum, Theory of high-harmonic generation by low-frequency laser fields, Phys. Rev. A **49**, 2117 (1994).

[44] P. M. Kraus, O. I. Tolstikhin, D. Baykusheva, A. Rupenyan, J. Schneider, C. Z. Bisgaard, T. Morishita, F. Jensen, L. B. Madsen, and H. J. Wörner, Observation of laser-induced electronic structure in oriented polyatomic molecules, Nat. Commun. **6**, 7039 (2015).

[45] A. Etches and L. B. Madsen, Extending the strong-field approximation of high-order harmonic generation to polar molecules: Gating mechanisms and extension of the harmonic cutoff, J. Phys. B **43**, 155602 (2010).

[46] A. Etches, M. B. Gaarde, and L. B. Madsen, Laser-induced bound-state phases in high-order-harmonic generation, Phys. Rev. A **86**, 023818 (2012).

[47] M. Spanner and S. Patchkovskii, One-electron ionization of multielectron systems in strong nonresonant laser fields, Phys. Rev. A **80**, 063411 (2009).

[48] A.-T. Le, R. R. Lucchese, S. Tonzani, T. Morishita, and C. D. Lin, Quantitative rescattering theory for high-order harmonic generation from molecules, Phys. Rev. A **80**, 013401 (2009).

[49] P. Salières, A. Maquet, S. Haessler, J. Caillat, and R. Taïeb, Imaging orbitals with attosecond and Ångström resolutions: toward attochemistry? Rep. Prog. Phys. **75**, 062401 (2012).

[50] C. Leone, S. Bivona, R. Burlon, F. Morales, and G. Ferrante, Gauge aspects in multichannel multiphoton ionization, Phys. Rev. A **40**, 1828 (1989).

[51] M. F. Ciappina, C. C. Chirilă, and M. Lein, Influence of Coulomb continuum wave functions in the description of high-order harmonic generation with H_2^+, Phys. Rev. A **75**, 043405 (2007).

[52] Y. J. Chen and Bambi Hu, Strong-field approximation for diatomic molecules: Comparison between the length gauge and the velocity gauge, Phys. Rev. A **80**, 033408 (2009).